

Thermo-acoustical study of biologically active 1,1'-bis(3-methyl-4-carboxyethylphenoxy) cyclohexane at four different temperatures

Bhavin B. Dhaduk, P. H. Parsania*

Polymer Chemistry Division, Department of Chemistry, Saurashtra University,
Rajkot - 360 005, Gujarat, India

*E-mail address: phparsania22@gmail.com

ABSTRACT

Density (ρ), viscosity (η), ultrasonic speed (U), and thermo-acoustical parameters such as specific acoustical impedance (Z), adiabatic compressibility (κ_a), internal pressure (π), free volume (V_f), inter molecular free path length (L_f), Van der Waals constant (b), viscous relaxation time (τ), classical absorption coefficient ($(\alpha/f^2)_{cl}$), Rao's molar sound function (R_m), solvation number (S_n), Gibbs free energy of activation (ΔG^*), enthalpy of activation (ΔH^*) and entropy of activation (ΔS^*) of biologically active 1,1'-bis(3-methyl-4-carboxyethylphenoxy)cyclohexane (BMCP) in 1,4-dioxane (DO), ethyl acetate (EA), tetrahydrofuran (THF) have been studied at four different temperatures: 298, 303, 308 and 313 K to understand the molecular interactions in the solutions. A good to excellent correlation between a given parameter and concentration is observed at all temperatures and solvent systems studied. Linear increase or decrease [except $(\alpha/f^2)_{cl}$] of acoustical parameters with concentration and temperature indicated the existence of strong molecular interactions. ΔG^* decreased linearly with increasing concentration and temperature in DO and EA systems and increased with temperature in THF system. ΔH^* and ΔS^* are found practically concentration independent in case of DO and EA system but both are found concentration dependent in THF system

Keywords: Ultrasonic speed; acoustical parameters; thermodynamic parameters

1. INTRODUCTION

“Ultrasonic sound” refers to sound waves of such a high frequency that they cannot be heard. These waves are also known as silent sound waves having frequencies beyond the range of human hearing i.e. above 20 KHz (20,000 cycles per second). These waves are also part of a characterization technique of a fluid. A fluid can be defined as a substance that deforms continuously under the action of a shear stress of any amount. Fluid properties can be characterized by variables such as pressure, velocity, density, and temperature. These properties will form a continuous function of position/time and therefore the fluid can be treated as a continuum. Ultrasonic sound is a viable technology because it is readily available and can be used for wide range of applications in different fields including consumer industries, pharmaceutical industries, medical field, process industries and chemical industries etc [1–4].

Recently ultrasonic sound radiations are used in synthetic organic chemistry, which cause a decrease of reaction time, increase of yield, lower reaction temperature, and avoidance of phase transfer catalysis [5–7]. Further ultrasonic sound velocity measurements have been used to study the nature of molecular interactions in various liquid mixtures and solution of organic and inorganic compounds [8-10], solutions of polymers [11,12], pharma materials [13, 14] and ionic interactions in electrolytes solutions [15,16].

To the best of our knowledge no work has been reported on ultrasonic speed and related acoustical parameters of biologically active 1,1'-bis(3-methyl-4-carboxyethylphenoxy) cyclohexane (BMPCP) (Figure 1). In present work we have reported measurement of density, viscosity, ultrasonic speed and related thermo-acoustical parameters of biologically active 1, 1'-bis(3-methyl-4-carboxyethylphenoxy) cyclohexane in 1, 4-dioxane (DO), ethyl acetate (EA), tetrahydrofuran (THF) solutions (0.01 to 0.1 M) at four different temperatures: 298, 303, 308 and 313 K. The derived parameters are correlated with concentration in different solvents and at different temperatures.

2. EXPERIMENTAL DETAILS

2.1. Materials

1,1'-Bis(3-methyl-4-carboxyethylphenoxy) cyclohexane (BMPCP) used in this study was synthesized and crystallized according to our recent publication [17]. 1, 4-Dioxane (DO), ethyl acetate (EA) and tetrahydrofuran (THF) were supplied by Spectrochem Pvt. Ltd. Mumbai and were purified according to literature methods [18]. The density (ρ), viscosity (η) and ultrasonic speed (U) of pure solvents were compared with the literature values [19-29] and are shown in Table 1.

2.2. Measurements

0.1 M fresh stock solutions of 1,1'-bis(3-methyl-4-carboxyethylphenoxy)cyclohexane (BMPCP) was prepared in DO, EA and THF at room temperature. From the stock solutions a series of dilute solutions ranging from 0.1 to 0.01 M were prepared and thermally equilibrated at specified temperatures prior to density, viscosity and ultrasonic speed measurements. The ρ and U measurements were carried out on a Density and Sound Velocity Meter (DSA-5000 M) supplied by Anton Paar, Gmbh, Graz, Austria. The repeatability in density, ultrasonic speed, and temperature measurements were $\pm 1 \cdot 10^{-6} \text{ kg} \cdot \text{m}^{-3}$, $\pm 1 \cdot 10^{-1} \text{ m} \cdot \text{s}^{-1}$, and $\pm 1 \cdot 10^{-3} \text{ K}$, respectively. The standard uncertainties for the density, ultrasonic speed, and temperatures were better than $2.9 \cdot 10^{-2} \text{ kg} \cdot \text{m}^{-3}$, $1.3 \cdot 10^{-1} \text{ m} \cdot \text{s}^{-1}$, and $1 \cdot 10^{-2} \text{ K}$, respectively. The calibration of DSA-5000 was done over a temperature range from 25–40 °C. DSA-5000 was thermostated within $\pm 0.002 \text{ }^\circ\text{C}$ with Peltier heating device. Viscometric measurements were carried out by using Ubbelohde type viscometer. The repeatability in the viscosity measurements was $\pm 0.1 \%$. The viscosity measurements were repeated at least three times for each sample. A constant temperature bath (Nova Instruments, Ahmedabad, Model NV8550E) with an accuracy of $\pm 0.1 \text{ K}$ was used for maintaining constant temperature during viscosity measurements. The flow times of pure solvents and solutions were measured with a digital RACER HS 10W stop watch with an accuracy of $\pm 0.01 \text{ s}$. The solutions were prepared by mass using an analytical balance (AB 204-S; Mettler Toledo, Switzerland) with an uncertainty of $\pm 1 \cdot 10^{-4} \text{ kg}$.

2.3. Data processing

Various acoustical and thermodynamic parameters were determined according to following theoretical equations:

Specific acoustical impedance (Z):

$$Z = U\rho \quad (1)$$

Adiabatic compressibility (κ_a):

$$\kappa_a = \frac{1}{U^2\rho} \quad (2)$$

Internal pressure (π) [30]:

$$\pi = b'RT \left(\frac{K'\eta}{U} \right)^{\frac{1}{2}} \frac{\rho^{2/3}}{M^{7/6}} \quad (3)$$

Where b' is the packing factor (2), K' is a constant (4.28×10^9) and R is the gas constant $\{8.314 / (\text{JK}^{-1} \text{mol}^{-1})\}$.

Free volume (V_f) [30]:

$$V_f = \left[\frac{MU}{K\eta} \right]^{3/2} \quad (4)$$

Inter molecular free path length (L_f) [31]:

$$L_f = K_J(\kappa_a)^{1/2} \quad (5)$$

Where K_J is the Jacobson's constant [$K = (93.875 + 0.375T) \times 10^{-8}$] and it is temperature dependent.

Van der Waals constant (b) [32]:

$$b = \frac{M}{\rho} \left[1 - \left[\frac{RT}{MU^2} \right] \left[\sqrt{1 + \frac{MU^2}{3RT}} - 1 \right] \right] \quad (6)$$

Where M is the apparent molecular weight of the solution, R is the gas constant and T is the absolute temperature.

Viscous relaxation time (τ) :

The resistance offered by viscous force in the flow of sound wave appears as a classical absorption associated with it is the viscous relaxation time:

$$\tau = \frac{4\eta}{3\rho U^2} \quad (7)$$

Classical absorption coefficient $(\alpha/f^2)_{cl}$ [33]:

$$\left(\frac{\alpha}{f^2}\right)_{cl} = \frac{8\pi^2\eta}{3U^3\rho} \quad (8)$$

Rao's molar sound function [34]:

$$R_m = \frac{M}{\rho} U^{1/3} \quad (9)$$

Solvation number (S_n):

The number of grams of solvent connected in the apparent solvation of 1 g of solute assuming the solvent molecules participating in the solvation are effectively incompressible due to strong localized electronic fields is expressed as:

$$n = \left[1 - \frac{\kappa_a(100-X)}{\kappa_{a_1}X} \right] \quad (10)$$

Where X is the number of grams of solute in 100 g of the solution.

The solvation number (S_n) can be expressed as:

$$S_n = \frac{M_2}{M_1 \left(1 - \frac{\kappa_a}{\kappa_{a_1}} \right) \left(\frac{100-X}{X} \right)} \quad (11)$$

Where M_1 and M_2 are the molecular weights of solvent and solute, respectively.

Thermodynamic parameters:

Free energy of activation (ΔG^*), enthalpy of activation (ΔH^*) and entropy of activation (ΔS^*) can be determined by using viscous relaxation time data at different concentrations and temperatures:

$$\frac{1}{\tau} = \frac{kT}{h} e^{-\frac{\Delta G^*}{RT}} \quad (12)$$

$$\ln \frac{1}{\tau T} = \ln \frac{k}{h} + \frac{\Delta S^*}{R} - \frac{\Delta H^*}{RT} \quad (13)$$

Where k is the Boltzmann constant and h is the Planck's constant.

3. RESULTS AND DISCUSSION

3.1. Density, viscosity and ultrasonic speed

Experimentally derived quantities such as ρ , η and U of pure solvents: DO, EA, THF and BMCPC solutions at four different temperatures: 298, 303, 308 and 313 K are presented in Table 2. The densities of BMCPC solutions increased linearly with concentration (C) and decreased linearly with temperature because of rule of additivity indicating that the density of BMCPC is greater than those of solvents used in the present study. Both η and U of BMCPC solutions increased linearly with C and decreased with T. The ρ , η and U data were correlated with C and T, and excellent correlation of these parameters with C and T is found (regression coefficient R^2 0.9914-0.999). The variation of η and U with C and T are considerably more than that of ρ due to specific solvent and solute interactions. The nature of solvent and the solute play an important role on molecular interactions such as association, dissociation, H-bonding, etc. occurring in the solutions. Strong intermolecular H-bond formation is expected in THF system as compared to EA and DO. Thus, THF has more solvating tendency than EA and DO. Solvation causes change in apparent molecular mass and volume of the compound and hence change in density, viscosity and ultrasonic speed.

Various acoustical and thermodynamic parameters such as specific acoustical impedance (Z), adiabatic compressibility (κ_a), internal pressure (π), free volume (V_f), inter molecular free path length (L_f), Van der Waals constant (b), viscous relaxation time (τ), classical absorption coefficient (αf^2)_{cl}, Rao's molar sound function (R_m), solvation number (S_n), Gibbs free energy of activation (ΔG^*), enthalpy of activation (ΔH^*) and entropy of activation (ΔS^*) of BMCPC solutions were derived according to above mentioned theoretical relations and were correlated with C and T. The least-squares equations along with regression coefficients (R^2) are reported in Tables 3-5 from which it is observed that excellent correlation between a given parameter and concentration of BMCPC is found at different temperatures.

Both U and Z increased with C and decreased with T due to strong molecular interactions. κ_a of solutions is decreased with C and increased with T in all solvents. This can be attributed to the fact that the solvated molecules were fully compressed by the electrical forces of the solute. The strong solvent-solute interactions lead to compressibility. Variation of U in the solution depends upon intermolecular free path length. Due to molecular association (solvent-solute interactions) compressibility of the solution is decreased with the increasing solute concentration. Inter molecular free path length is inversely proportional to ultrasonic speed. It was observed from the results that L_f decreased with C and increased with T further supported the presence of strong molecular interactions. The presence of solvent - solute interactions can also be confirmed from dispersion of ultrasonic speed, which is characterized by relaxation process. According to Eyring rate theory τ is inversely proportional to temperature and hence, increased in the temperature of system caused to decrease in relaxation process. τ is decreased with C and T. R_m and b increased with C and T indicated that no complex formation taken place in all the systems. The internal pressure (π) decreased with C and increased with T. The results of π also confirmed our observations for κ_a and L_f . The internal pressure (π) decreased with C and increased with T. The results of π also confirmed our observation for κ_a and L_f , which are temperature dependent. The internal pressure depends on temperature, density, ultrasonic speed and specific heat at a

constant pressure, while L_f is temperature dependent. A variation in the values of π is due to different orientations of BMAPC in DO, EA and THF. The free volume (V_f) is inversely proportional to the internal pressure and *vice-versa*. The ordered structural arrangement is due to decreasing entropy of the system.

Solvation phenomenon results into modification of the structure of the solution. The plots of S_n against C for BMCPC at different temperatures are presented in Figures 2-4 from which it is observed that S_n increased nonlinearly with C and decreased with T indicating competing solvent-solute and solute-solute interactions in the solutions. Thus, S_n values also supported stronger molecular interactions. Minimum solvation is observed in case of DO system. The lone pairs of electrons of THF, DO, ester group of EA interact with ether, ester and methyl groups of BMCPC and structural modification takes place in the solutions. Due to the structural modification both apparent molecular mass and molecular volume found to change and consequently the density, viscosity and ultrasonic speed in the solutions also changed.

When ultrasonic waves are incident on the solution, the molecules get perturbed. Since the medium has some elasticity and hence perturbed molecules regain their equilibrium positions. When a solute is added to a solvent, its molecules attract certain solvent molecules toward them. The phenomenon is known as compression and also as limiting compressibility. The aggregation of solvent molecules around solute molecules supports strong solvent-solute interactions and considerable change in structural arrangement. Molecular interactions such as solvent-solute interactions, quantum mechanical dispersive forces and dielectric force may cause high degree of contraction or expansion. The time lag between the excitation and de-excitation processes is observed as an acoustical relaxation. This relaxation process is observed as either an increase in speed with frequency or a decrease in the $(\alpha/f^2)cl$ with frequency.

Increasing temperature has two opposite effects namely structure formation (intermolecular association) and structure destruction. The structure forming tendency is primarily due to solvent-solute interactions, while destruction of structure formed previously is due to thermal fluctuations. When thermal energy is greater than that of interaction energy, it causes destruction of the structure formed previously [11, 12]. Dipole-dipole interactions of the opposite type favours structure formation, while of the same type favour structure breaking tendency. The decreasing cohesive forces lead to increasing free length and free volume of the system.

Thermodynamic parameters such as ΔG^* , ΔH^* and ΔS^* were determined according to Eqns. 12 and 13 using viscous relaxation time data as a function of concentration and temperature are shown in Table 6. In DO system, ΔG^* decreased with increasing C (R^2 0.993-0.998) and T, while both ΔH^* and ΔS^* are found practically concentration independent. In EA and THF systems, ΔG^* decreased linearly with increasing C (R^2 0.990-0.999) and increased linearly with increasing T, In EA system it remained practically constant with increasing C. In THF system both ΔH^* and ΔS^* are found concentration dependent. Derived thermodynamic parameters indicated that condensation and evaporation processes are concentration and temperature dependent. The negative values of ΔH^* and ΔS^* indicated that activated complexes are highly in ordered state, i.e. condensation process is predominant over evaporation process, which is further supported by positive values of S_n with C. Thus, thermodynamic parameters supported presence of strong molecular interactions occurring in the solutions of different polarity

Table 1. Comparison of measured density (ρ), viscosity (η) and ultrasonic speed (U) data for DO, EA and THF with literature values at 298, 303, 308 and 313 K.

T (K)	ρ ($\text{kg}\cdot\text{m}^{-3}$)		η ($\text{m}\cdot\text{Pa}\cdot\text{s}$)		U ($\text{m}\cdot\text{s}^{-1}$)	
	expt	Lit	Expt	Lit	Expt	Lit
DO						
298	1027.60	1027.99 ^a	1.222	1.212 ^a	1344.87	1345.1 ^a
303	1021.82	1022.33 ^a	1.094	1.115 ^a	1322.99	1323.1 ^a
308	1016.21	1016.36 ^a	1.010	1.028 ^a	1301.14	1301.3 ^a
313	1010.46	1010.97 ^a	0.927	0.952 ^a	1279.42	1279.7 ^a
EA						
298	894.79	894.81 ^f 894.6 ^g	0.427	0.421 ^f 0.424 ^g	1140.53	1137.7 ^h
303	888.65	887.14 ^f 888.5 ^g	0.405	0.399 ^f 0.400 ^g	1118.07	1115.3 ^h
308	882.47	882.21 ^f 882.5 ^g	0.384	0.381 ^f 0.385 ^g	1095.64	1093.0 ^h
313	876.23	878.92 ^f	0.364	0.363 ^f	1073.41	1070.7 ^h
THF						
298	882.33	882.50 ⁱ 882.01 ^j	0.463	0.459 ⁱ 0.449 ^j	1278.30	1278.24 ^j
303	876.83	877.0 ^k	0.4466	0.42 ^k	1254.25	1254.00 ^k
308	871.34	-	0.4305	-	1230.27	-
313	865.03	865.93 ⁱ 861.2 ^k	0.4133	0.4007 ⁱ 0.39 ^k	1206.46	1202.00 ^k

^a Reference [19]. ^b Reference [20]. ^c Reference [21]. ^d Reference [22]. ^e Reference [23]. ^f Reference [24].

^g Reference [25]. ^h Reference [26]. ⁱ Reference [27]. ^j Reference [28]. ^k Reference [29]

Table 2. The density (ρ), viscosity (η), and ultrasonic speed (U) data for BMCPC in DO, EA and THF at 298 K, 303 K, 308 K and 313 K.

Conc. ^a ($\text{mol}\cdot\text{L}^{-1}$)	Density ρ^b / ($\text{kg}\cdot\text{m}^{-3}$)				Viscosity η^c / ($\text{mPa}\cdot\text{s}$)				Ultrasonic speed U^d / ($\text{m}\cdot\text{s}^{-1}$)			
	298 K	303 K	308 K	313 K	298 K	303 K	308 K	313 K	298 K	303 K	308 K	313 K
DO + BMCPC												
0.00	1027.6	1021.8	1016.2	1010.5	1.2224	1.0939	1.0100	0.9269	1344.9	1323.0	1301.1	1279.4
0.01	1028.1	1022.5	1016.9	1011.2	1.2234	1.0948	1.0109	0.9280	1345.3	1323.3	1301.4	1279.8

0.02	1028.6	1023.2	1017.6	1011.9	1.2257	1.0961	1.0125	0.9293	1347.0	1324.2	1302.4	1280.7
0.04	1029.5	1024.5	1018.9	1013.2	1.2271	1.0984	1.0143	0.9313	1347.3	1325.4	1303.6	1282.2
0.06	1030.5	1025.9	1020.3	1014.7	1.2299	1.1008	1.0166	0.9335	1348.6	1326.8	1305.1	1283.5
0.08	1031.5	1027.2	1020.6	1016.0	1.2324	1.1033	1.0190	0.9358	1350.1	1328.2	1306.5	1285.0
0.10	1032.7	1028.6	1023.0	1017.4	1.2353	1.1064	1.0221	0.9385	1351.8	1330.0	1308.3	1286.8
EA+ BMCPC												
0.00	894.8	888.7	882.5	876.2	0.4274	0.4045	0.3846	0.3644	1140.5	1118.1	1095.6	1073.4
0.01	895.5	889.5	883.2	877.0	0.4283	0.4060	0.3854	0.3651	1142.5	1119.1	1096.8	1074.5
0.02	896.7	890.5	884.4	878.2	0.4292	0.4071	0.3865	0.3661	1143.0	1120.5	1098.1	1076.0
0.04	898.8	892.7	886.6	880.4	0.4310	0.4091	0.3882	0.3676	1145.5	1123.3	1100.9	1078.7
0.06	901.7	895.0	888.9	882.7	0.4327	0.4111	0.3901	0.3693	1148.4	1125.9	1103.7	1081.7
0.08	903.2	897.1	891.0	884.9	0.4346	0.4133	0.3921	0.3713	1151.2	1128.7	1106.4	1084.3
0.10	905.5	899.4	893.4	887.3	0.4369	0.4157	0.3945	0.3736	1154.9	1131.4	1109.2	1087.3
THF+ BMCPC												
0.00	882.3	876.8	871.3	865.7	0.4625	0.4474	0.4299	0.4129	1278.3	1254.3	1230.3	1206.5
0.01	884.4	879.0	873.4	867.9	0.4641	0.4489	0.4316	0.4149	1279.7	1255.7	1231.9	1208.2
0.02	885.9	880.4	874.9	869.3	0.4653	0.4500	0.4331	0.4164	1280.7	1256.9	1233.0	1209.2
0.04	888.8	883.4	877.9	872.4	0.4676	0.4520	0.4356	0.4192	1283.0	1259.0	1235.3	1211.8
0.06	891.5	886.1	880.6	875.1	0.4696	0.4543	0.4382	0.4217	1285.0	1261.3	1237.6	1214.1
0.08	894.4	889.0	883.5	878.0	0.4715	0.4568	0.4410	0.4245	1287.4	1263.6	1240.0	1216.7
0.10	897.6	892.2	886.7	881.2	0.4741	0.4598	0.4439	0.4273	1289.6	1266.1	1242.5	1219.1

Table 3. The least-square equations and regression coefficients for BMCPC solutions in DO at 298 K, 303 K, 308 K and 313K.

Parameter	Least square equations (regression coefficients, R^2) [DO+ BMCPC]			
	298 K	303 K	308 K	313 K
ρ ($\text{kg}\cdot\text{m}^{-3}$) ^a	66.04 C + 1027 (0.999)	67.08 C + 1021 (0.999)	68.08 C + 1016 (0.999)	69.15 C + 1010 (0.999)
η ($\text{m}\cdot\text{Pa}\cdot\text{s}$) ^b	0.1255 C + 1.2224 (0.991)	0.1245 C + 1.0936 (0.997)	0.118 C + 1.0098 (0.995)	0.1142 C + 0.9268 (0.998)
U ($\text{m}\cdot\text{s}^{-1}$) ^a	95.35 C + 1346 (0.999)	98.51 C + 1324 (0.999)	100.8 C + 1302 (0.999)	102.9 C + 1280 (0.999)
$Z \times 10^{-6}$ ($\text{kg}\cdot\text{m}^{-2}\cdot\text{s}^{-1}$) ^c	0.1359 C + 1.382 (0.993)	0.1612 C + 1.3516 (0.999)	0.1622 C + 1.3219 (0.999)	0.1636 C + 1.2926 (0.999)
$\kappa_a \times 10^{10}$	-0.7859 C + 5.3803	-0.9512 C + 5.5934	-1.0219 C + 5.815	-1.0975 + 6.0473

$(\text{Pa}^{-1})^d$	(0.9888)	(0.998)	(0.998)	(0.9991)
$L_f \times 10^{11}$	-0.356 C + 4.8566	-0.4228 C + 4.9518	-0.4456 C + 5.049	-0.4694 C + 5.4188
$(\text{m})^e$	(0.9888)	(0.998)	(0.998)	(0.9991)
$R_m \times 10^4$	15.733 C + 9.4653	15.63 C + 9.4659	15.711 C + 9.466	15.789 C + 9.4663
$(\text{m}^{10/3} \cdot \text{s}^{-1/3} \cdot \text{mol}^{-1})^f$	(1)	(1)	(1)	(1)
$b \times 10^5$	13.662 C + 8.0779	13.624 C + 8.1137	13.757 C + 8.1487	13.885 C + 8.1845
$(\text{m}^3)^g$	(1)	(1)	(1)	(1)
$\pi \times 10^{-8}$	-8.7163 C + 5.3333	-8.3847 C + 5.1525	-8.2632 C + 5.0561	-8.1071 C + 4.9453
$(\text{Pa})^h$	(0.998)	(0.9977)	(0.998)	(0.998)
$V_f \times 10^7$	2.7565 C + 1.077	3.1736 C + 1.2415	3.5069 C + 1.3646	3.9003 C + 1.5134
$(\text{m}^3)^i$	(1)	(1)	(1)	(1)
$\tau \times 10^{13}$	-0.3941 C + 8.7696	-0.4746 C + 8.1561	-0.4771 C + 7.8267	-0.4524 C + 7.4734
$(\text{s})^j$	(0.981)	(0.995)	(0.996)	(0.996)
$(\alpha/f^2)_{cl} \times 10^{15}$	-1.2073 C + 12.858	-1.3462 C + 12.159	-1.3741 C + 11.869	-1.3521 C + 11.52
$(\text{s}^2 \text{m}^{-1})^k$	(0.979)	(0.995)	(0.997)	(0.997)
	-1E+09 C ⁵ + 3E+08 C ⁴ - 3E+07 C ³ + 1E+06 C ² - 24933 C + 156	-2E+06 C ⁴ + 314584 C ³ - 12274 C ² + 381.98 C + 16.852	-1E+06 C ⁴ + 182013 C ³ - 2445 C ² + 86.372 C + 19.064	-852961 C ⁴ + 148780 C ³ - 6417.6 C ² + 439.54 C + 12.438
Sn^l	(1)	(0.996)	(0.997)	(0.991)

Table 4. The least-square equations and regression coefficients for BMCPC solutions in EA at 298 K, 303 K, 308 K and 313K.

Parameter	Least square equations (regression coefficients, R^2) [EA+ BMCPC]			
	298 K	303 K	308 K	313 K
ρ	66.04 C + 1027	67.08 C + 1021	68.08 C + 1016	69.15 C + 1010
$(\text{kg} \cdot \text{m}^{-3})^a$	(0.999)	(0.999)	(0.999)	(0.999)
η	0.0934 C + 0.4573	0.1061 C + 0.4049	0.0976 C + 0.3845	0.0904 C + 0.3642
$(\text{m} \cdot \text{Pa} \cdot \text{s})^b$	(0.998)	(0.999)	(0.997)	(0.994)
U	95.35 C + 1346	98.51 C + 1324	100.8 C + 1302	102.9 C + 1280
$(\text{m} \cdot \text{s}^{-1})^a$	(0.999)	(0.999)	(0.999)	(0.999)
$Z \times 10^{-6}$	0.2519 C + 1.0199	0.2433 C + 0.9932	0.2432 C + 0.9665	0.2434 C + 0.9401
$(\text{kg} \cdot \text{m}^{-2} \cdot \text{s}^{-1})^c$	(0.998)	(0.999)	(0.999)	(0.999)
$\kappa_a \times 10^{10}$	-3.1041 C + 8.5982	-3.2046 C + 9.0059	-3.4573 C + 9.4441	-3.7434 C + 9.9096
$(\text{Pa}^{-1})^d$	(0.998)	(0.999)	(0.999)	(0.999)
$L_f \times 10^{11}$	-1.1184 C + 6.1396	-1.1279 C + 6.2834	-1.1886 C + 6.4345	-1.2567 C + 6.5912
$(\text{m})^e$	(0.998)	(0.999)	(0.999)	(0.999)
$R_m \times 10^4$	19.004 C + 10.291	19.107 C + 10.294	19.237 C + 10.297	19.374 C + 10.3
$(\text{m}^{10/3} \cdot \text{s}^{-1/3} \cdot \text{mol}^{-1})^f$	(1)	(1)	(1)	(1)
$b \times 10^5$	17.116 C + 9.2035	17.319 C + 9.2531	17.526 C + 9.3039	17.74 C + 9.3554
$(\text{m}^3)^g$	(0.999)	(0.999)	(0.999)	(0.999)
$\pi \times 10^{-8}$	-5.5416 C + 3.1196	-5.485 C + 3.1041	-5.5077 C + 3.0912	-5.5214 C + 3.0742
$(\text{Pa})^h$	(0.997)	(0.997)	(0.997)	(0.996)
$V_f \times 10^7$	11.742 C + 4.0628	11.997 C + 4.2822	12.776 C + 4.4898	13.633 C + 4.7221
$(\text{m}^3)^i$	(1)	(1)	(1)	(0.9999)
$\tau \times 10^{13}$	-0.7367 C + 4.8994	-0.5012 C + 4.8627	-0.5876 C + 4.8417	-0.6679 C + 4.8125
$(\text{s})^j$	(0.994)	(0.994)	(0.992)	(0.986)
$(\alpha/f^2)_{cl} \times 10^{15}$	-2.2999 C + 8.4732	-1.898 C + 8.5774	-2.1218 C + 8.715	-2.3479 C + 8.8421
$(\text{s}^2 \text{m}^{-1})^k$	(0.996)	(0.9982)	(0.998)	(0.995)
	-3E+06 C ⁴ + 521833 C ³ - 33353 C ² + 969.86 C + 2.7983 C	-2E+06 C ⁴ + 472708 C ³ - 32260 C ² + 995.37 C + 2.114	-3E+06 C ⁴ + 543776 C ³ - 37010 C ² + 1107.9 C + 1.1364	-4E+06 C ⁴ + 737107 C ³ - 47909 C ² + 1308.4 C + 1.1364
Sn^l	(0.991)	(0.99)	(0.9896)	(1)

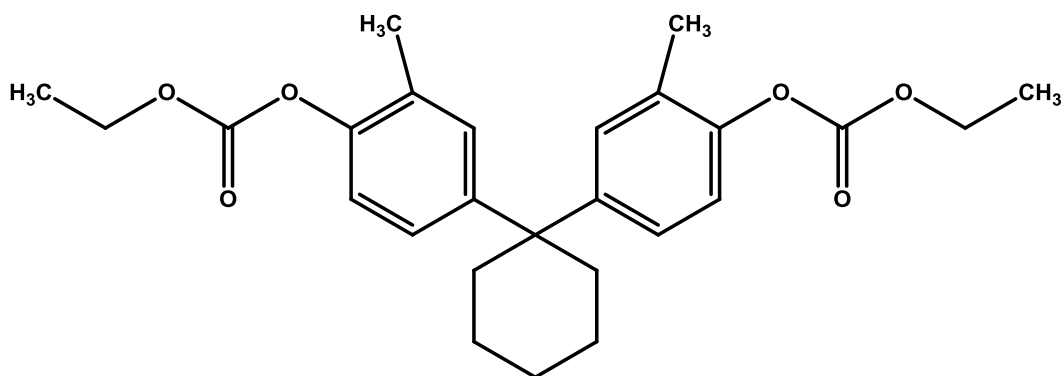
Table 5. The least-square equations and regression coefficients for BMCPC solutions in THF at 298 K, 303 K, 308 K and 313K.

Parameter	Least square equations (regression coefficients, R^2) [THF+ BMCPC]			
	298 K	303 K	308 K	313 K
ρ ($\text{kg}\cdot\text{m}^{-3}$) ^a	66.04 C + 1027 (0.999)	67.08 C + 1021 (0.999)	68.08 C + 1016 (0.999)	69.15 C + 1010 (0.999)
η ($\text{m}\cdot\text{Pa}\cdot\text{s}$) ^b	0.1118 C + 0.4629 (0.997)	0.1196 C + 0.4474 (0.996)	0.1366 C + 0.4301 (0.999)	0.1399 C + 0.4134 (0.998)
U ($\text{m}\cdot\text{s}^{-1}$) ^a	95.35 C + 1346 (0.999)	98.51 C + 1324 (0.999)	100.8 C + 1302 (0.999)	102.9 C + 1280 (0.999)
$Z \times 10^{-6}$ ($\text{kg}\cdot\text{m}^{-2}\cdot\text{s}^{-1}$) ^c	0.2887 C + 1.1285 (0.999)	0.2098 C + 1.1004 (0.999)	0.29 C + 1.0726 (0.999)	0.2909 C + 1.0452 (0.999)
$\kappa_a \times 10^{10}$ (Pa^{-1}) ^d	-2.3132 + 6.9305 (0.999)	-2.5061 C + 7.2437 (0.999)	-2.7061 C + 7.5758 (0.999)	-2.9339 C + 7.9276 (0.998)
$L_f \times 10^{11}$ (m) ^e	-0.9275 C + 5.5121 (0.999)	-0.9832 C + 5.6352 (0.999)	-1.0383 C + 5.763 (0.999)	-1.1008 C + 5.8953 (0.998)
$R_m \times 10^4$ ($\text{m}^{10/3}\cdot\text{s}^{-1/3}\cdot\text{mol}^{-1}$) ^f	20.674 C + 8.8715 (1)	20.802 C + 8.8709 (1)	20.93 C + 8.8702 (1)	21.062 C + 8.8695 (1)
$b \times 10^5$ (m^3) ^g	18.119 C + 7.6424 (1)	18.315 C + 7.6793 (1)	18.516 C + 7.7167 (1)	18.722 C + 7.7547 (1)
$\pi \times 10^{-8}$ (Pa) ^h	-8.2901 C + 3.8295 (0.996)	-8.3421 C + 3.8487 (0.995)	-8.3301 C + 3.8564 (0.995)	-8.3611 C + 3.8628 (0.995)
$V_f \times 10^7$ (m^3) ⁱ	11.628 C + 3.1714 (1)	11.831C + 3.2438 (1)	11.986 C + 3.3443 (1)	12.344 C + 3.4475 (0.9999)
$\tau \times 10^{13}$ (s) ^j	-0.4284 C + 4.2777 (0.994)	-0.3793 C + 4.3221 (0.973)	-0.2205 C + 4.3454 (0.983)	-0.1911 C + 4.37 (0.975)
$(\alpha/f^2)_{cl} \times 10^{15}$ (s^2m^{-1}) ^k	-1.2245 C + 6.5979 (0.998)	-1.2129 C + 6.7941 (0.993)	-1.0201 C + 6.9635 (0.996)	-1.0359 C + 7.141 (0.998)
Sn^l	-4E+06 C ⁴ + 858859 C ³ - 65747 C ² + 2261.1 C - 8.9486 (0.9585)	-5E+06 C ⁴ + 1E+06 C ³ - 79845 C ² + 2581.3 C + 11.595 (0.9815)	-5E+06 C ⁴ + 1E+06 C ³ - 88776 C ² + 2827.6 C - 13.692 (0.981)	-5E+06 C ⁴ + 1E+06 C ³ - 80784 C ² + 2645 C - 12.453 (0.955)

Table 7. Thermodynamic parameters (ΔG^* , ΔH^* and ΔS^*) derived using τ data for BMAPC in DO, EA and THF solutions.

System	Conc.	$\Delta G^* / (\text{J mol}^{-1})^a$				$\Delta H^* /$ (kJ mol^{-1})	$\Delta S^* /$ ($\text{J K}^{-1} \text{mol}^{-1}$)
		298 K	303 K	308 K	313 K		
DO+ BMCPC	0.01	4199.0	4196.4	4133.8	4119.5	5.56	4.63
	0.02	4196.4	4193.9	4132.3	4117.8	5.54	4.57
	0.04	4195.6	4191.7	4128.8	4114.2	5.60	4.76
	0.06	4193.4	4188.4	4125.3	4111.5	5.60	4.80
	0.08	4191.1	4185.4	4122.4	4107.7	5.63	4.89
	0.1	4187.9	4182.2	4119.3	4104.9	5.62	4.87
EA+ BMCPC	0.01	2753.5	2870.3	2900.7	2972.8	-1.65	-14.75
	0.02	2749.5	2868.0	2898.4	2969.4	-1.66	-14.80
	0.04	2742.9	2862.0	2890.5	2959.8	-1.61	-14.59
	0.06	2734.2	2855.6	2883.7	2950.7	-1.60	-14.55
	0.08	2726.9	2850.8	2877.4	2946.0	-1.65	-14.68
	0.1	2718.0	2846.2	2873.7	2941.0	-1.73	-14.94

	0.01	2416.9	2568.5	2624.2	2722.5	-3.56	-20.07
	0.02	2415.7	2565.5	2624.4	2723.2	-3.65	-20.37
	0.04	2410.8	2559.7	2620.7	2720.4	-3.76	-20.69
THF+ BMPCP	0.06	2405.9	2555.3	2618.3	2717.6	-3.81	-20.86
	0.08	2398.9	2552.0	2616.6	2715.3	-3.91	-21.17
	0.1	2395.5	2549.7	2613.3	2712.4	-3.92	-21.19



1,1'-Bis(3-methyl-4-carboxyethylphenoxy)cyclohexane

Chemical formula: $C_{26}H_{32}O_6$

Molar Mass: 440.53

Fig. 1. Structure of 1,1'-Bis(3-methyl-4-carboxyethylphenoxy)cyclohexane (BMPCP).

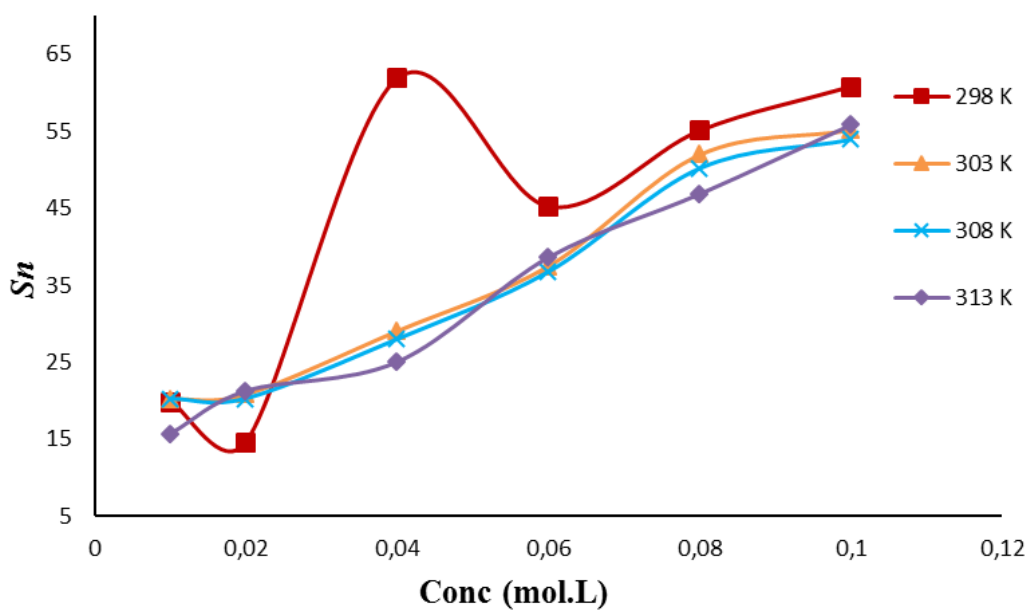


Fig. 2. The plots of solvation number (S_n) against concentration (C) for BMPCP in DO at 298K (■), 303 K (▲) and 308 K (×), 313 K (◇).

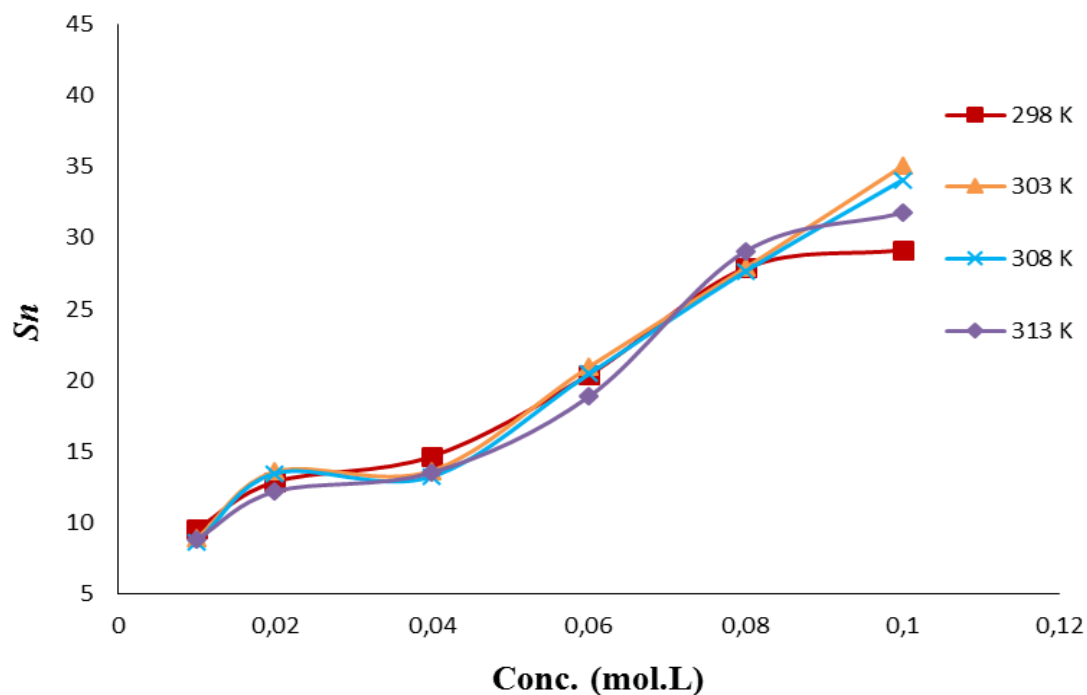


Fig. 3. The plots of solvation number (S_n) against concentration (C) for BMCPC in EA at 298K (■), 303 K (▲) and 308 K (×), 313 K (◇).

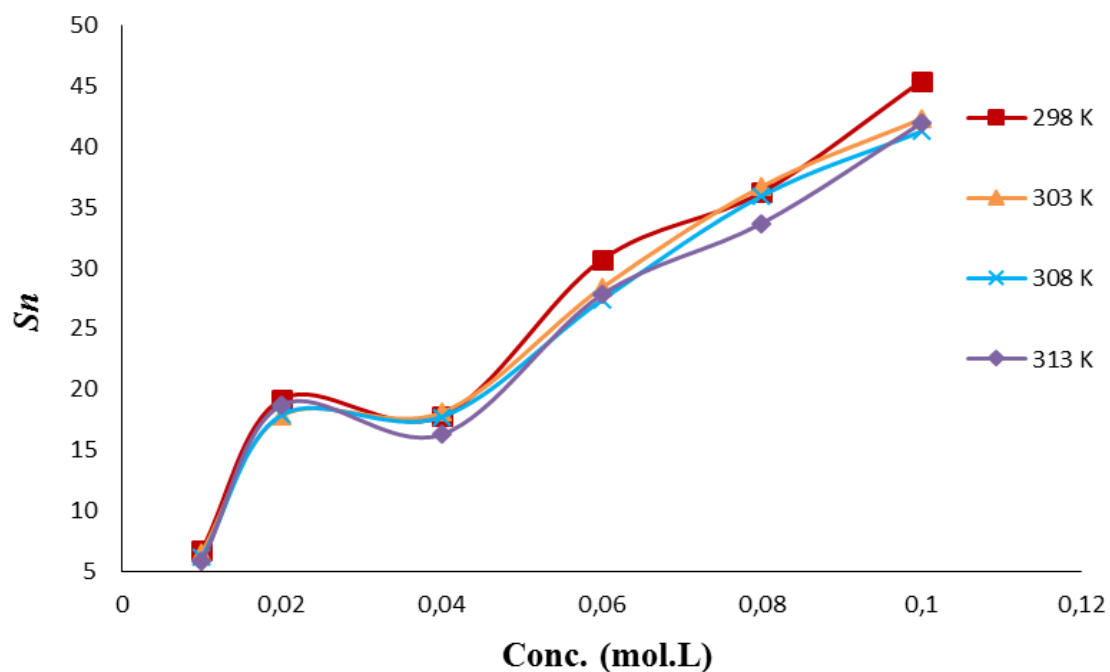


Fig. 4. The plots of solvation number (S_n) against concentration (C) for BMCPC in THF at 298K (■), 303 K (▲) and 308 K (×), 313 K (◇).

4. CONCLUSIONS

Excellent correlation between studied acoustical and thermodynamic parameters with concentration and temperature was observed. Derived acoustical and thermodynamic parameters confirmed existence of strong molecular interactions in the solutions. ΔG^* is decreased with increasing concentration of BMCPC in all the system studied. ΔH^* and ΔS^* are found concentration independent in DO and EA but they are concentration dependent in THF system.

Acknowledgements

The authors are thankful to UGC-SAP, New Delhi and DST-FIST, New Delhi for the instrumentation grants. Bhavin is thankful to UGC-New Delhi for BSR Fellowship in Science.

References

- [1] T. J. Mason, *Sonochemistry: The uses of ultrasound in chemistry*. Royal Soc. of Chem., (1990).
- [2] T. N. Pashovkin, D. G. Sadikova, M. S. Pashovkin, G. V. Shilnikov, *Bull. Exp. Bio Med.* 144 (2007) 118-122.
- [3] B. A. Scheven, R. M. Shelton, P. R. Cooper, A. D. Walmsley, A. J. Smith, *Med. Hypotheses*. 73 (2009) 591-593.
- [4] A. Carovac, F. Smajlovic, D. Junuzovic, *Acta. Inform. Med.* 19 (2011), 168-171.
- [5] Price, G. J., *Current Trends in Sonochemistry*, Royal Society of Chemistry, Cambridge, 1992
- [6] M. Mexiarova, M. Kiripolsky, S. Toma, *Ultra. Sonochem.* 12 (2005) 401-403.
- [7] C. E. Sherlock, T. S. Mari, T. F. Braake, *Vet. Radio Ultrasound*, 50 (2009) 13-20.
- [8] S. J. Askar Ali, *J. Chem. Pharm. Res.* 4 (2012) 617-632.
- [9] S. Baluja, F. Karia, *J. Chem. Bio. Phys. Sci. Sec. A.* 2 (2012) 101-107.
- [10] S. Nishikawa, *J. Phys. Chem. B.* 117 (2013) 896-900.
- [11] B. D. Bhuvu, P.H. Parsania, *J. Sol. Chem.* 40 (2011) 719-726.
- [12] U. G. Pathak, J. V. Patel, P. H. Parsania, *J. Sol. Chem.* 41 (2012) 755-765.
- [13] M. Levina, M. H. Rubinstein, *J. Pharm. Sci.* 89 (2000) 705-723.
- [14] M. Enriquez-Sarano, V. T. Nkomo, H. Michelena, *Card. Surg. Adult.* 3 (2008) 315-348.
- [15] K. Jerie, A. Baranowski, J. Przybylski, J. Gliński, *Phys. Lett. A.* 323(2004) 148-153.
- [16] B. R. Shinde, K. M. Jadhav, *J. Eng. Res. Stud.* 1 (2010) 128-137.
- [17] B. B. Dhaduk, C. B. Patel, P.H. Parsania, *Lett. Drug. Des. Discov.* 12 (2015), 152-157.

-
- [18] A. I. Vogel, A. R. Tatchell, B. S. Furnis, A. J. Hannaford, P. W.G. Smith, *Vogel's Textbook of Practical Organic Chemistry, 5th edn.*, Addison Wesley Longman, London 395 (1998).
- [19] M. Habibullah, I. M. Rahman, M. A. Uddin, M. Anowar, M. Alam, K. Iwakabe, H. Hasegawa, *J. Chem. Eng. Data* 58 (2013) 2887-2897.
- [20] R. A. Clará, A. C. Gómez Marigliano, D. Morales, H. N. Sólamo, *J. Chem. Eng. Data* 55 (2010) 5862-5867.
- [21] M. N. Sovilj, *J. Chem. Eng. Data* 40 (1995) 1058-1061.
- [22] U. B. Kadam, A. P. Hiray, A. B. Sawant, M. Hasan, *J. Chem. Eng. Data* 51 (2006) 60-63.
- [23] G. Savaroğlu, E. Aral, *J. Mol. Liq.* 105 (2003) 79-92.
- [24] H. Djojoputro, S. Ismadji, *J. Chem. Eng. Data* 50 (2005) 727-731.
- [25] P. S. Nikam, T. R. Mahale, M. Hasan, *J. Chem. Eng. Data* 41 (1996) 1055-1058.
- [26] J. Resa, C. Gonzalez, J. Goenaga, M. Iglesias, *Phys. Chem. Liq.* 43 (2005) 65-89.
- [27] A. Mariano, A. Camacho, M. Postigo, A. Valen, H. Artigas, F. Royo, J. Urieta, *J. Chem. Eng.* 17 (2000) 459-470.
- [28] M. T. Zafarani-Moattar, R. Majdan-Cegincara, *J. Chem. Eng. Data* 52 (2007), 2359-2364.
- [29] M. Gupta, I. Vibhu, J. Shukla, *Fluid Phase Equilibr.* 244 (2006) 26-32.
- [30] C. V. Suryanarayana, J. J. Kuppaswamy, *J. Acoust. Soc. India* 4 (1976) 75-82.
- [31] B. Jacobson, W. A. Anderson, J. T. Arnold, *Nature* 173 (1954) 772-773.
- [32] P. Vigoureux, *Ultrasonic*, Chapman and Hall, London, 112 (1952).
- [33] C.V. Suryanarayana, *J. Acoust. Soc. India* 5 (1977) 11-26.
- [34] S. Bagchi, S.K. Nema, R.P. Singh, *Eur. Polym. J.* 22 (1989) 851-860.

(Received 31 December 2014; accepted 12 January 2015)